INVITED PAPER Special Section on Distinguished Papers in Photonics

Pre-Equalizing Electro-Optic Modulator Utilizing Polarization-Reversed Ferro-Electric Crystal Substrate*

Hiroshi MURATA[†**a)], ***Member***, **Tomohiro OHNO**[†], **Takayuki MITSUBO**[†], ***Nonmembers***, ***and*** **Atsushi SANADA**[†], ***Senior Member***

SUMMARY We have proposed and developed new electro-optic modulators for the pre-equalization of signal distortion caused by the optical fiber chromatic dispersion effect. We found that the synthesis of an almost arbitrary impulse response function is obtainable by utilizing an electro-optic modulator composed of a Mach-Zehnder waveguide and travelling-wave electrodes on a ferro-electric material substrate with polarization-reversed structures. In this paper, the operational principle, design and simulation results of the pre-equalization modulator are presented. Some preliminary experimental results are also shown with future prospects.

key words: *optical modulator, Pockels effect, polarization reversal, impulse response, equalization*

1. Introduction

A single-mode silica optical fiber is indispensable for long haul communication networks in the world; a silica fiber has the lowest propagation loss in any kind of data transmission cable [1], [2] and a rather wide transmission bandwidth over THz with negligible crosstalk. Recently, study and development of multi-core and/or multi-mode optical fibers are also attracting a lot of interest for advanced communication networks [3], [4].

However, a silica fiber has one disadvantage for high-speed data transmission; it shows dispersion characteristics owing to material dispersion and structure dispersion. The dispersion effect essentially causes signal distortion since the phase relationship between frequency components are changed through fiber transmission.

Compensating for the optical signal distortion resulting from the chromatic dispersion of silica fibers is indispensable in modern long-haul telecommunication systems, since the signal distortion is proportional to the square of the data/symbol repetition frequency. Therefore, it is a big problem in high-data-density modulation formats which employ advanced vector modulation techniques.

In order to compensate for the signal distortion resulting from the chromatic dispersion effect, the digital coherent method utilizing high-speed analog-to-digital (A/D) converters and digital signal processors has been developed and implemented [5]–[8]. This technique is robust and applicable for any modulation format including vector modulation schemes. Despite this, there may be a power consumption issue; higher electrical power is necessary for signal processing and cooling as the bit-rate becomes faster. Dispersion compensation fibers are also applicable for the distortion compensation [9], [10]. However, their operational wavelength range is essentially limited.

We have proposed a high-speed pre-equalizing electro-optic modulator (EOM) utilizing velocity-mismatched traveling-wave electrodes and polarization-reversed substrates of ferro-electric optical crystals [11]–[13]. This pre-equalizing EOM is based on electrical-optical signal conversion with temporal convolution and the synthesis of an arbitrary impulse response, which enables us to obtain a complex transfer function precisely tuned to counter the signal distortion caused by fiber chromatic dispersion [8]. In this device, pre-equalization and electrical-optical signal conversion are obtained simultaneously without A/D conversion and high-speed signal processing. Therefore, dispersion compensation with low-power consumption can be obtained.

In this paper, the basic structure, operational principle, and some preliminary experimental results of the proposed EOM are presented.

2. Structure of Pre-Equalizing EOM

The basic structure of the proposed pre-equalizing EOM is shown in Fig. 1. A Mach-Zehnder (MZ) or double Mach-Zehnder (DMZ) optical waveguide is fabricated on a substrate of ferro-electric electro-optic (EO) crystals like $LiNbO_3$. EO polymer is also applicable although rather fine

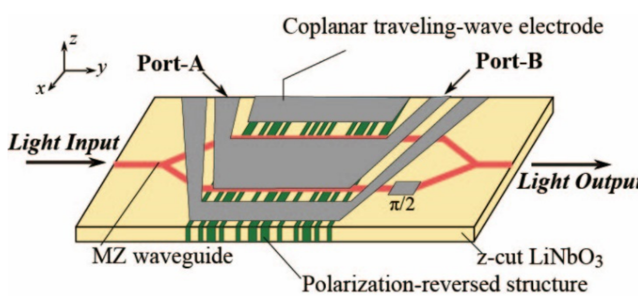

Fig. 1 Basic structure of the proposed pre-equalizing EO modulator.

Manuscript received November 7, 2017.
Manuscript revised February 16, 2018.
*This is an original article.
[†]The authors are with Graduate School of Engineering Science, Osaka University, Toyonaka-shi, 560–8531 Japan.
[**]Presently, with Graduate School of Engineering, Mie University.
a) E-mail: murata@elec.mie-u.ac.jp
DOI: 10.1587/transele.E101.C.581

(~50 μm) poling structures are necessary for the equalizing operation.

When standard digital amplitude-shift-keying (ASK) signals are supplied to the electrode of the modulator, electrical-to-optical signal conversion and pre-equalization are obtained simultaneously. Therefore, the output light signals from the device seem distorted, but after propagation through an optical fiber of a designed length, clear optical ASK signals are obtained.

By utilizing a DMZ waveguide rather than a standard MZ waveguide, pre-equalization for vector/IQ modulation signals (QPSK, QAM, and so on) is obtainable since the proposed pre-equalization scheme is based on a pair of high-speed optical phase modulation characteristics in a constellation plane [8]. By switching the input and output of the electrical signal, the extension of the fiber length to be compensated for is possible due to the electric signal counter-propagation with the lightwave [12].

3. Operational Principle

Figure 2 shows the basic operation block diagram for the equalization. The inverse transfer function of the optical fiber dispersion effect is implemented in the EOM by utilizing the transfer function synthesis technique with velocity-mismatched traveling-wave modulation and polarization-reversed structures [11].

For the case of a lightwave (LW) signal transfer over an optical fiber of length L_f, the transfer function can be expressed as follows,

$$H(\omega) = \exp(-j\beta(\omega)L_f) \tag{1}$$

where β is the propagation constant for the fundamental mode in the fiber and the optical loss through the fiber transfer is assumed to be sufficiently small. With the Taylor expansion of β at the angular frequency of the LW carrier, ω_0, β can be expressed as follows when the third and higher order dispersion effects are negligible.

$$\beta(\omega) = \beta_1(\omega - \omega_0) + \frac{1}{2}\beta_2(\omega - \omega_0)^2 \tag{2}$$

Therefore, the transfer function for the signal distortion caused by fiber dispersion is expressed as follows.

$$H_{dis}(\omega) = \exp\left(-\frac{1}{2}j\beta_2\omega^2 L_f\right) \tag{3}$$

Taking a Fourier transform of this dispersion transfer function, the impulse response of the LW signal distortion caused by fiber dispersion is obtained. Figure 3 shows calculated examples of the impulse response of the dispersion effect with the group velocity dispersion of D = 16 ps/(nm km) and the fiber length of L_f = 10 km. The real and imaginary parts of the impulse response of the fiber dispersion are plotted.

Then, the transfer function to compensate for the LW signal distortion caused by the fiber chromatic dispersion

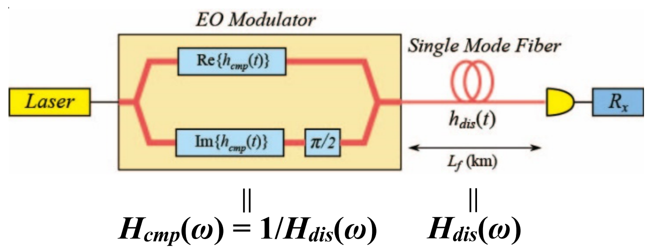

Fig. 2 Block diagram and basic operation of the proposed pre-equalization EOM.

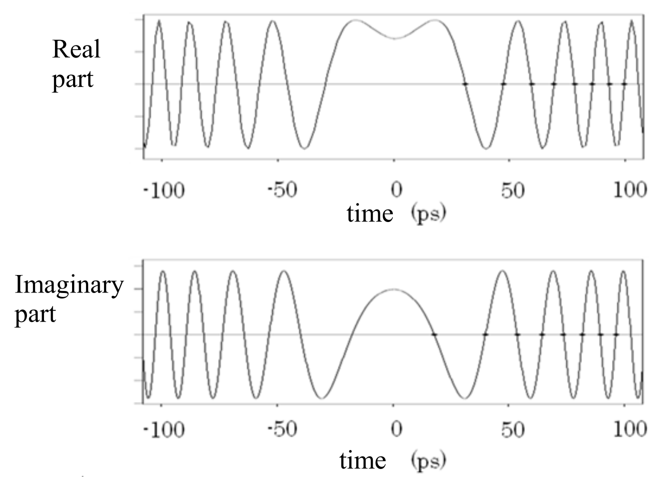

Fig. 3 Calculated example of the impulse response, $h(t)$, to express fiber dispersion effect. (D = 16 ps/(nm km) and L_f = 10 km)

effect is expressed as $H_{cmp}(\omega) = 1/H_{dis}(\omega) = H_{dis}{}^*(\omega)$. Therefore, by utilizing an EOM of impulse response, $h^*(-t)$, pre-equalization is obtainable with electrical-to-optical signal conversion simultaneously [11]. The required impulse response is a complex function. Therefore, the real part of the impulse function is set at one path in the MZ waveguide and the imaginary part is set at the other path in the MZ waveguide with an optical phase shift of $\pi/2$. By using this scheme, pre-equalization function can be implemented in the EOM. The impulse response $h^*(-t)$ is given by the Fourier transform of $H_{dis}{}^*(\omega)$.

$$\begin{aligned} h^*(-t) &= \frac{1}{2\pi}\int H_{dis}{}^*(\omega)\exp(j\omega t)\mathrm{d}t \\ &= \frac{1}{2\pi}\int \exp\left(\frac{1}{2}j\beta_2\omega^2 L_f\right)\exp(j\omega t)\mathrm{d}t \\ &= \frac{1}{\sqrt{2\pi\beta_2 L_f}}\exp\left\{j\left(-\frac{t^2}{2\beta_2 L} + \frac{\pi}{4}\right)\right\} \\ &= \frac{1}{\sqrt{2\pi\beta_2 L_f}}\left\{\cos\left(-\frac{t^2}{2\beta_2 L_f} + \frac{\pi}{4}\right)\right. \\ &\quad \left. + j\sin\left(-\frac{t^2}{2\beta_2 L_f} + \frac{\pi}{4}\right)\right\} \end{aligned} \tag{4}$$

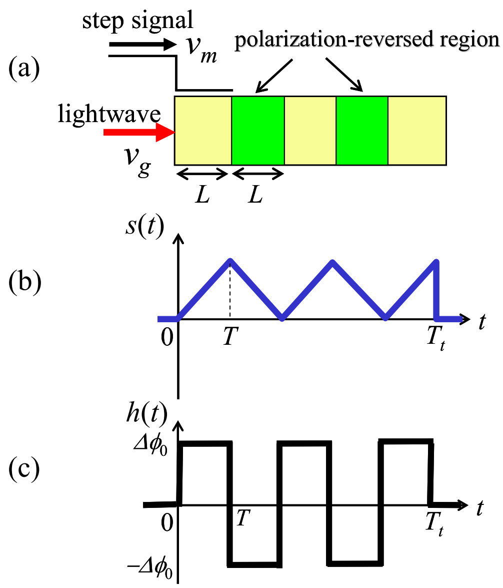

Fig. 4 (a) EO phase modulator with a traveling-wave electrode and polarization-reversed structures. (b) Its step response and (c) impulse response.

4. Design of the Pre-Equalization Modulator

In order to realize the pre-equalization operation, the reverse impulse response of the fiber dispersion effect should be implemented to the EOM. The impulse response of a travelling-wave electrode EOM can be calculated easily by a differential operation of its step response [14]. The step response of a travelling-wave electrode EOM is obtained with the simple consideration as shown in Fig. 4. Figure 4(a) shows a simple configuration of a travelling-wave electrode EOM with some polarization-reversed regions. Then, we assume that the group velocity v_g of the LW propagating in the optical waveguide is larger than the phase velocity v_m of the electrical signal travelling along the electrode and that dispersion and depletion of the modulation signal in the electrode are negligible. In this case, the step response becomes a triangle-like shape according to the polarization-reversed patterns as shown in Fig. 4(b). By differentiating the step response with time, the impulse signal response of this EO phase modulator is obtained (Fig. 4(c)).

Therefore, the impulse responses of the traveling-wave electrode EOM with polarization-reversed structures are obtained by simple digital-like shape functions corresponding to the polarization-reversed patterns themselves [6]. The temporal scale Δt in the impulse response is proportional to the spatial length ΔL of the electrode. Their relationship is calculated by use of the velocity difference between the LW propagating in the waveguide and the electric signal travelling along the electrode.

$$\Delta t = \frac{\Delta L}{c}|n_g - n_m| \tag{5}$$

where c is the LW velocity in vacuum, n_g is the group index of the LW propagating in the optical waveguide, and n_m is the effective refractive index of the electrical signal travelling along electrode. For example, when a standard channel optical waveguide in $LiNbO_3$ ($n_g \sim 2$) and a thin metal travelling-wave electrode ($n_m \sim 4$) are assumed, the corresponding temporal window for the convolution becomes $\Delta t = 200$ ps when the travelling-wave electrode length is $\Delta L = 30$ mm. This temporal window is proportional to the products of a signal bit-rate and a fiber length able to compensate for signal distortion using this EOM. For example, when a 40Gb/s NRZ ASK signal is supplied to this EOM with LW of 1.55 μm wavelength, the signal distortion can be compensated for after transmission of a standard single mode fiber ($D = 16$ ps/(nm km)) of 20 km long. In a 40 Gb/s RZ ASK signal case, clear signal can be obtained after 10km-long fiber propagation.

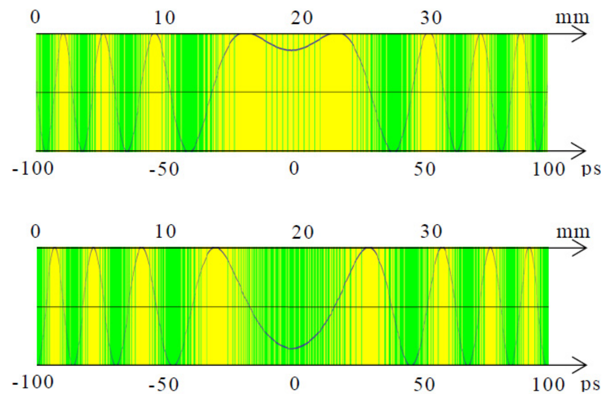

Fig. 5 Calculated impulse responses (solid lines) and corresponding polarization-reversed patterns in the $LiNbO_3$ crystal substrate for pre-equalization. (a) Real part. (b) Imaginary part.

Table 1 Parameters of the device design.

Light wavelength for compensation λ	1.55 µm
Modulation signal format	40 Gb/s ASK or BPSK
Fiber length to be compensated for L_f	10 km
Group velocity dispersion D	16 ps/(nm km)
Group index of the lightwave n_g	2.19
Effective index of the modulation signal n_m	3.98
Electrode length ΔL	38.25 mm
Minimum polarization-reversed length l_p	50 µm
Number of polarization-reversed regions N	~250

The designed polarization-reversed regions for the pre-equalization are shown as the green areas in Fig. 5. The black curves in Fig. 5 are the ideal impulse responses for pre-equalization calculated from Fig. 3. We can use the delta-sigma transformation technique to implement the required impulse responses by use of the fine polarization-reversed structures [12], [13]. These two patterns are to be set to the two paths in the MZ waveguide. The parameters of the designed EOM are summarized in Table 1.

The calculated example of the LW output signal envelopes from the designed EOM and its variation through

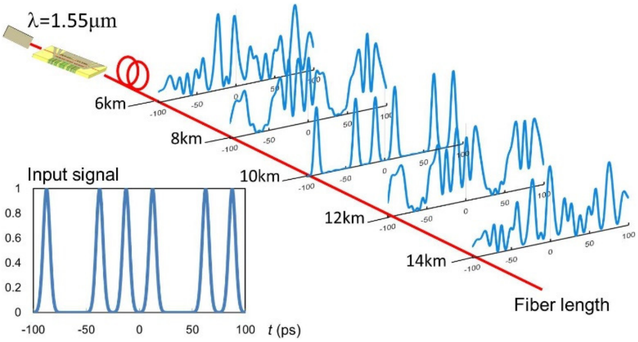

Fig. 6 Calculated variations of the LW signal from the designed EOM after optical fiber transmission. (D = 16 ps/(nm km)).

optical fiber transmission are plotted in Fig. 6 when a 40 Gb/s RZ ASK signal is supplied to the designed EOM with a 1.55 μm LW input. We can see that the signal distortion can be compensated for after 10 km transmission through a silica fiber.

5. Experiment

The designed pre-equalizing EOM was fabricated using a z-cut congruent $LiNbO_3$ wafer 250 μm thick with the standard device fabrication method. For the fabrication of the designed polarization-reversed structures, the pulse-voltage applying method was used. A MZ waveguide was fabricated by use of the annealed proton exchange method. The traveling-wave electrodes, where the characteristic impedance is matched with 50 Ω, but the microwave velocity (the effective index of the microwave signal n_m = 3.98) is not matched with the lightwave velocity (the group index of the lightwave n_g = 2.19) in order to obtain temporal convolution, were formed onto the MZ waveguide after the deposition of a 0.2-μm-thick SiO_2 buffer layer. The photograph of the fabricated EOM is illustrated in Fig. 7.

The performance of the fabricated pre-equalizing EOM was tested by use of the experimental set-up shown in Fig. 8. We measured the transfer function response of the fabricated pre-equalizing EOM by utilizing the variable dispersion compensator (VIPA [10], [11]), which can generate optical dispersion effects equivalent to 0 to 20 km-long silica fiber cables. From a microwave oscillator, a single-tone microwave signal from 8 to 24 GHz was supplied to the fabricated pre-equalizing EOM. The output signal from the pre-equalizing EOM was fed to the VIPA, and then the output from the VIPA was detected by use of a fast photodiode. A typical example of the measured results is shown in Fig. 9. For comparison, the results using a standard MZ EOM are also shown. In the fabricated pre-equalizing EOM, the output power levels were enhanced for all the measured frequency when a dispersion effect corresponding to a 10-km-long fiber was applied by the VIPA. While, for the standard MZ EOM case, the signal distortion resulting from the dispersion effect was shown periodically at each frequency. These figures were in line with our expected results. Therefore, the synthesis of the transfer function utilizing polarization reversed structures and velocity-mismatched travelling-wave electrode was verified.

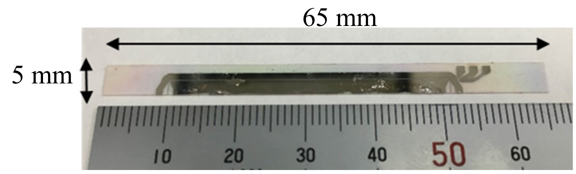

Fig. 7 Photograph of the fabricated pre-equalization EO modulator.

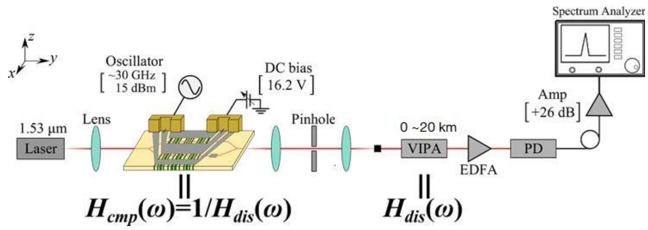

Fig. 8 Experimental set-up for the measurement of the transfer function of the EO modulator.

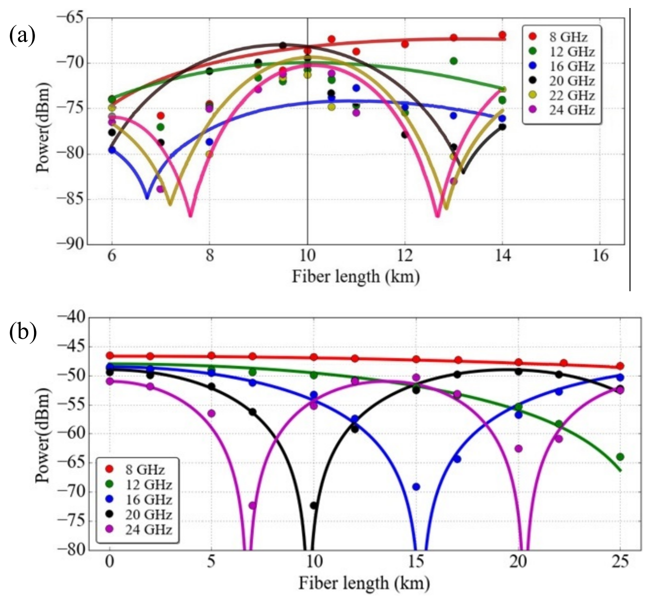

Fig. 9 Measured output signal levels for the single tone-modulation operation with changing the equivalent fiber length by user of the variable dispersion compensator (VIPA). (a) The fabricated pre-equalizing EOM. (b) Commercially available standard MZ EOM.

6. Conclusion

The pre-equalization EOM utilizing the velocity-mismatched electrodes and the polarization-reversed structures is discussed. Although the polarization reversal changes only the sign of EO interaction digitally, useful signal processing characteristics are obtainable with the combination of the temporal delay in high-speed EO modulation devices. These techniques are also applicable for EO polymer devices and semiconductor-based EO devices.

The proposed EOM is operated as a pre-equalizer for the designed fixed fiber length with the fixed dispersion parameter. However, by adopting the structure for loading a metal plate or a dielectric plate with an appropriate dielectric constant, we can tune the fiber length/dispersion constant to be compensated for in the range of −20 % to +10 % [12].

Acknowledgments

The authors thank Dr. Hidehisa Shiomi, Dr. Toshiyuki Inoue, Mr. Kouhei Iida of Osaka University, Japan, Dr. Atsushi Kanno of NICT, Japan and Dr. Kensuke Ikeda of CRIEPI, Japan for their valuable comments and supports about the device design and experiments.

References

[1] G. Keiser, "Optical Fiber Communication," Wiley 2003.
[2] Y. Tamura, H. Sakuma, K. Morita, M. Suzuki, Y. Yamamoto, K. Shimada, Y. Honma, K. Sohma, T. Fujii, and T. Hasegawa, "Lowest-Ever 0.1419-dB/km Loss Optical Fiber," Proc. OFC 2017 Post-deadline paper Th5D.1, Los Angeles, CA, USA, March 2017.
[3] B.J. Puttnam, R.S. Luís, W. Klaus, J. Sakaguchi, J.-M.D. Mendinueta, Y. Awaji, N. Wada, Y. Tamura, T. Hayashi, M. Hirano, and J. Marciante, "2.15 Pb/s transmission using a 22 core homogeneous single-mode multi-core fiber and wideband optical comb," Proc. ECOC 2015, Post-deadline paper PDP3.1, Valencia, Spain, Oct. 2015.
[4] J. Sakaguchi, B.J. Puttnam, W. Klaus, Y. Awaji, N. Wada, A. Kanno, T. Kawanishi, K. Imamura, H. Inaba, K. Mukasa, R. Sugizaki, T. Kobayashi, and M. Watanabe, "19-core fiber transmission of 19x100x172-Gb/s SDM-WDM-PDM-QPSK signals at 305Tb/s," Proc. OFC 2012, Post-deadline paper PDP5C.1, Los Angeles, CA, USA, March 2012.
[5] K. Kikuchi, "Digital coherent optical communication systems: fundamentals and future prospects," IEICE ELEX, vol.8, no.20, pp.1642–1662, 2011.
[6] S. Tsukamoto, K. Katoh, and K. Kikuchi, "Unrepeated transmission of 20-Gb/s optical quadrature phase-shift-keying signal over 200-km standard single-mode fiber based on digital processing of homodyne-detected signal for group-velocity dispersion compensation," IEEE Photon. Technol. Lett., vol.18, pp.1016–1018, 2006.
[7] S. Savory, "Digital signal processing for coherent systems," Proc. OFC 2012, OTh3C-7, Los Angeles, CA, USA, March 2012.
[8] R.I. Killey, P.M. Watts, V. Mikhailov, M. Glick, and P. Bayvel, "Electronic dispersion compensation by signal predistortion using digital processing and a dual-drive Mach–Zehnder modulator," IEEE Photon. Tech. Lett., vol.17, no.3, pp.714–716, 2005.
[9] T.A. Birks, D. Mogilevtsev, J.C. Knight, and P.S.J. Russell, "Dispersion compensation using single-material fibers," IEEE Photon. Tech. Lett., vol.11, no.6, pp.674–676, 1999.
[10] B.J. Eggleton, B. Mikkelsen, G. Raybon, A. Ahuja, J.A. Rogers, P.S. Westbrook, T.N. Nielsen, S. Stulz, and K. Dreyer, "Tunable dispersion compensation in a 160-Gb/s TDM system by a voltage controlled chirped fiber bragg grating," IEEE Photon. Tech. Lett., vol.12, no.8, pp.1022–1024, 2000.
[11] H. Murata and Y. Okamura, "High-Speed Signal Processing Utilizing Polarization-Reversed Electro-Optic Devices," IEEE/OSA J. Lightwave Technol., vol.32, pp.3403–3410, 2014.
[12] T. Ohno, H. Murata, and Y. Okamura, "Improved Equalizing Characteristics in Pre-equalizing Electro-Optic Modulator with Polarization-Reversed Structures," Proc. the 21st Optoelectronics and Communications Conference/International Conference on Photonics in Switching 2016 (OECC/PS 2016), TuD2-2, July 2016, Niigata, Japan.
[13] T. Ohno, H. Murata, and A. Sanada, "Electro-Optic Modulator for Pre-Equalization of Fiber Chromatic Dispersion Utilizing Travelling-Wave Electrodes and Polarization-Reversed Structures," Proc. Microwave Photonics 2017 (MWP2017), Th1.3, Beijing, China, Oct. 2017.
[14] M. Izutsu and T. Sueta, "Picosecond pulse response of broad-band guided-wave interferometric light modulators," IEEE J. Quantum Electron., vol.QE-19, no.4, pp.668–674, 1983.
[15] M. Shirasaki, "Variable dispersion compensation using the virtually imaged phased array (VIPA) for 40-Gbit/s WDM transmission systems," Proc. ECOC2000, Post-deadline paper PDP2.3, Munich, Germany, Sept. 2000.
[16] H. Ooi, K. Nakamura, Y. Akiyama, T. Takahara, T. Terahara, Y. Kawahata, H. Isono, and G. Ishikawa "40-Gb/s WDM transmission with virtually imaged phased array (VIPA) variable dispersion compensators," J. Lightwave Technol., vol.20, no.12, pp.2196–2203, 2002.
[17] T. Ohno, H. Murata, and Y. Okamura, "Improvement of Equalizing Characteristics in Pre-equalizing Electro-Optic Modulator Using Polarization-Reversed Structures," IEICE Technical report (in Japanese), OPE2015-210, vol.115, no.432, pp.383–388, 2016.

Hiroshi Murata received the B.Eng., M.Eng., and D.Eng. degrees in electrical engineering from Osaka University in 1988, 1990, and 1998, respectively, for studies on analyses on nonlinear-optic guided-wave systems and its applications to all-optical devices. In 1991, he joined the Department of Electrical Engineering, Faculty of Engineering Science, Osaka University, where he was an Associate Professor in Division of Advanced Electronics and Optical Science until the end of March 2018. In 2018, he joined the Graduate School Engineering, Me University, Mie, Japan, where he is now a Professor. His works are concerned with electro optics, integrated optics, nonlinear optics and microwave-wave photonics. Dr. Murata is a member of the Institute of Electrical and Electronics Engineers (IEEE), The Optical Society (OSA), the European Microwave Association (EuMA), the Japan Society of Applied Physics, the Optical Society of Japan (OSJ), the Institute of Laser Engineering, and the Institute of Electronics, Information and Communication Engineers (IEICE).

Tomohiro Ohno received the B.Eng. and M.Eng. degrees in electrical engineering from Osaka University in 2015, and 2017, respectively, for studies on the pre-equalizing electro-optic modulator. In 2017, he joined West Japan Railway Company.

Takayuki Mitsubo received the B.Eng. and M.Eng. degrees in electrical engineering from Osaka University in 2013, and 2015, respectively, for studies on the pre-equalizing electro-optic modulator.

Atsushi Sanada received the B.Eng., M.Eng., and D.Eng. degrees in electronic engineering from Okayama University, Okayama, Japan, in 1989, 1991, and 1994, respectively. In 2016, he joined the Graduate School of Engineering Science, Osaka University, Osaka, Japan, where he is now a Professor. He was a Visiting Scholar with the University of California at Los Angeles in 1994–1995 and 2002–2003. He was also a Visiting Scholar with the Advanced Telecommunications Research Institute International in 2004–2005 and the Japan Broadcasting Corporation in 2005. His research is concerned with microwave science and technologies including transformation electromagnetics, metamaterials, high- Tc superconducting devices, and ferrite devices. Dr. Sanada is also a member of the Institute of Electrical and Electronics Engineers (IEEE) and the European Microwave Association (EuMA). He is currently serving as an elected member of the Administrative Committee of the Microwave Theory and Techniques Society (MTT-S) since 2015.